4330–4339 *Nucleic Acids Research, 2016, Vol. 44, No. 9* *Published online 20 April 2016*
doi: 10.1093/nar/gkw295

Pif1 is a force-regulated helicase

Jing-Hua Li[1,†], Wen-Xia Lin[1,†], Bo Zhang[2], Da-Guan Nong[1], Hai-Peng Ju[1], Jian-Bing Ma[1], Chun-Hua Xu[1], Fang-Fu Ye[1], Xu Guang Xi[2,3], Ming Li[1], Ying Lu[1,*] and Shuo-Xing Dou[1,*]

[1]Beijing National Laboratory for Condensed Matter Physics and CAS Key Laboratory of Soft Matter Physics, Institute of Physics, Chinese Academy of Sciences, Beijing 100190, China, [2]College of Life Sciences, Northwest A & F University, Yangling, Shaanxi 712100, China and [3]LBPA, ENS de Cachan, CNRS, Université Paris-Saclay, F-94235 Cachan, France

Received September 28, 2015; Revised April 7, 2016; Accepted April 8, 2016

ABSTRACT

Pif1 is a prototypical member of the 5′ to 3′ DNA helicase family conserved from bacteria to human. It has a high binding affinity for DNA, but unwinds double-stranded DNA (dsDNA) with a low processivity. Efficient DNA unwinding has been observed only at high protein concentrations that favor dimerization of Pif1. In this research, we used single-molecule fluorescence resonance energy transfer (smFRET) and magnetic tweezers (MT) to study the DNA unwinding activity of *Saccharomyces cerevisiae* Pif1 (Pif1) under different forces exerted on the tails of a forked dsDNA. We found that Pif1 can unwind the forked DNA repetitively for many unwinding-rezipping cycles at zero force. However, Pif1 was found to have a very limited processivity in each cycle because it loosened its strong association with the tracking strand readily, which explains why Pif1 cannot be observed to unwind DNA efficiently in bulk assays at low protein concentrations. The force enhanced the unwinding rate and the total unwinding length of Pif1 significantly. With a force of 9 pN, the rate and length were enhanced by more than 3- and 20-fold, respectively. Our results imply that the DNA unwinding activity of Pif1 can be regulated by force. The relevance of this characteristic of Pif1 to its cellular functions is discussed.

INTRODUCTION

Helicases are enzymes that can translocate along single-stranded nucleic acids and unwind double-stranded nucleic acids (1–3). They participate in most nucleic acid transactions, including DNA replication, recombination, repair, transcription and ribonucleoprotein assembly and remodeling (4–8). Pif1 belongs to the SF1 superfamily of helicases and nucleic acid translocases and has been found in the entire eukaryotic phylum, from yeast to human (9,10). It is a 5′-3′ helicase and plays an important role in the maintenance of both mitochondrial and nuclear genome stability (10–13). It prefers forked DNA molecules rather than nonforked molecules (14–16) for unwinding and has an unwinding step size of 1 bp and a low processivity of about 10 bp (16). Although it does not interact with RNA (15), it unwinds RNA/DNA hybrids better than dsDNA, and is also involved in the maintenance of telomeric DNA (17–20). Biochemical characterizations have shown that Pif1 exists as a monomer in solutions and dimerizes upon binding to DNA (14,21). Recently, it was shown that Pif1 monomers display some unwinding activity, but the unwinding efficiency is low (22).

Despite intensive research, Pif1 remains an enigmatic helicase with three fundamental puzzles. (i) Pif1 has a high affinity for DNA (13) but unwinds DNA efficiently only at relatively high protein concentrations. The high affinity of Pif1 for DNA is in accordance with the suggestion that the concentration of Pif1 in cells is low (14,23); even a moderate overproduction of Pif1 would induce a replication stress at telomeres (24). Given the low expression level of Pif1 and considering that it has an observable unwinding activity only at high concentrations, one might wonder whether cells use Pif1 as a helicase *in vivo*. (ii) Although Pif1 can translocate on ssDNA and knock off a streptavidin bound to the ssDNA (16,22,25), it is still a low or nonprocessive helicase (14,16). The second puzzle is hence what hinders Pif1 from unwinding dsDNA processively. (iii) Pif1 has been implicated in various replication processes, such as Okazaki fragment maturation (OFM) (26–31) and break-induced replication (BIR) (32,33). In the former process, Pif1 is involved in the extension of flaps from the 5′ end of the Okazaki fragments and the displacement activity of the DNA polymerase Pol δ. It promotes the formation of flaps that are long enough for Dna2 to process. In the meanwhile, it is not allowed to displace longer stretches of DNA; otherwise,

*To whom correspondence should be addressed. Tel: +86 10 8264 8122; Fax: +86 10 8264 0224; Email: yinglu@iphy.ac.cn
Correspondence may also be addressed to Shuo-Xing Dou. Tel: +86 10 8264 9484; Fax: +86 10 8264 0224; Email: sxdou@iphy.ac.cn
†These authors contributed equally to the paper as first authors.

all the downstream Okazaki fragments would be removed from the template unnecessarily. In the latter process, Pif1 strongly stimulates Pol δ-mediated DNA synthesis from the D-loops produced by the Rad51 recombinase. It liberates the newly synthesized strands to prevent the accumulation of topological constraint and facilitates extensive DNA synthesis via the establishment of a migrating D-loop that can copy tens of kilobases. The third (and also the biggest) puzzle is thus how the same helicase plays a role in the different processes that require different processivities.

By using smFRET, as well as MT that allow for real-time monitoring of DNA unwinding at different forces, we found that the Pif1 was able to unwind a DNA hairpin repetitively for many cycles at low Pif1 concentrations. The previously observed low unwinding activity resulted from extremely low processivity (< 10 bp) (induced by Pif1's frequent loosening of its strong association with the tracking strand during DNA unwinding). Interestingly, we found that both the unwinding rate and the processivity increased significantly with force. According to our results, Pif1 unwinds a short stretch of DNA in the OFM process, where the 5′ flap is tension free, and unwinds a long stretch of DNA at the synthesis front in a D-loop where the bending of dsDNA exerts a force on the ssDNA. We propose that Pif1 is a force-regulated helicase. Our results provide a mechanistic insight into how Pif1 modulates its helicase activity in different processes in cells.

MATERIALS AND METHODS

Buffers

The Pif1 reaction buffer contained 5 mM $MgCl_2$, 50 mM NaCl in 25 mM Tris-HCl, pH 7.5 with 2 mM DTT. For smFRET measurements, an oxygen scavenging system, 0.8% D-glucose, 1 mg/ml glucose oxidase (266 600 units/g, Sigma), 0.4 mg/ml catalase (2000–5000 units/mg, Sigma) and 1 mM Trolox, was added to the reaction buffer (34).

Pif1 purification

The plasmid encoding yeast Pif1 gene was kindly provided by Dr Zakian. The protein expression and purification were performed essentially according to Ref. (15) with minor modifications.

DNA constructs

All oligonucleotides required to make the DNA substrates were purchased from Sangon Biotech (Shanghai, China). For FRET assays, DNA was annealed by incubating the mixture at 95°C for 5 min, and then slowly cooled down to room temperature in about 7 h. The annealing was carried out in an annealing buffer containing 50 mM NaCl, 25 mM Tris-HCl, pH 7.5. For MT assays, the DNA substrates were constructed as described in Ref. (35).

Single-molecule fluorescence data acquisition and analyses

The smFRET study was carried out with a home-built objective-type total internal reflection fluorescence microscopy (34). Cy3 was excited by a 532 nm Sapphire laser (Coherent Inc., USA). An oil immersion objective (100×, N.A.1.49) was used to generate an evanescent field of illumination. The fluorescence signals from Cy3 and Cy5 were split by a dichroic mirror, and finally collected by an electron-multiplying charge-coupled device camera (iXON, Andor Technology, South Windsor, CT, USA). The fluorescence imaging process was controlled and recorded by MetaMorph (Molecular Devices, CA, USA). The coverslips (Fisher Scientific, USA) and slides were cleaned thoroughly by rinsing with acetone, methanol, a mixture of sulfuric acid and hydrogen peroxide with a volume ratio of 7:3 and then sodium ethoxide. The surfaces of coverslip were coated with a mixture of 99% mPEG (m-PEG-5000, Laysan Bio, Inc.) and 1% biotin-PEG (biotin-PEG-5000, Laysan Bio, Inc.). Streptavidin was added to the microfluidic chamber made of the PEG coated coverslip, and incubated for 10 min. After washing, 100 pM DNA was added to the chamber and immobilized for 10 min. Free DNA molecules were removed by washing the chamber with the reaction buffer. Then, the chamber was filled with the reaction buffer. The imaging was initiated before Pif1 and ATP were flowed into the chamber. An exposure time of 100 ms was used for all the single-molecule measurements, which were carried out at a constant temperature of 22°C. The raw fluorescence intensity trajectories were three-point averaged. Then, the FRET efficiency was calculated by using $I_A/(I_D+I_A)$, where I_D and I_A represent the intensity of the donor and the acceptor, respectively.

Single-molecule assays with MT

A flow chamber was assembled with a glass slide and a coverslip, and was placed on an inverted microscope (IX71, Olympus). Both slides were cleaned, and the coverslip was modified with anti-digoxigenin protein. A magnetic bead was tethered to the modified coverslip through a single DNA substrate. An external magnetic force was applied on the magnetic bead by placing a permanent magnet above the chamber. The distance between the magnetic bead and the coverslip, that is, the DNA extension, was monitored by analyzing the shape of the diffraction rings of the magnetic bead (36), which depends on the distance between the bead and the focal plane of the objective (100×, NA 1.45, Olympus). A stack of calibration images that recorded the shape of the diffraction rings versus distance was obtained by stepping the focal plane through a series of positions. After checking the state of the DNA-magnetic bead connection, the Pif1 helicase was injected into the chamber. The DNA unwinding events were monitored by recording the magnetic bead-surface distance, that is, the DNA extension, as a function of time. The DNA extension change at a certain force can be converted into the number of base pairs unwound by using the force versus extension curve of single-stranded DNA, which is well described by the freely jointed chain model at low forces (37).

RESULTS

With no external force, Pif1 unwinds DNA repetitively but with a low processivity

To study the Pif1 unwinding kinetics in the absence of external force, we performed smFRET assay using a forked duplex DNA substrate (Figure 1A). The duplex length was 40 bp, and the 3′ and 5′ Poly(dT) ssDNA overhangs had lengths of 15 and 26 nt, respectively. The donor (Cy3) and the acceptor (Cy5) were attached, respectively, to the two DNA strands at the ss/dsDNA junction. After incubation of the DNA with 2 nM Pif1 for 10 min, the free proteins in the chamber were washed away by the reaction buffer. The unwinding reaction was then initiated upon addition of ATP. Interestingly, we observed repetitive changes of FRET. A typical time trace of the FRET signal at 20 μM ATP is shown in Figure 1B. The bursting might repeat more than 50 times and usually lasted for an average of 2 min until the dye was photobleached. The unwinding burst was characterized by a gradual decrease followed by an abrupt recovery of the FRET signal, with the former attributed to the Pif1-catalyzed unwinding of the DNA duplex and the latter caused by the spontaneous rezipping of the unwound DNA after Pif1 loosened its strong association with the 5′ tracking strand. It should be noted that previous studies have shown that the placement of the fluorophores at the junctions does not affect the unwinding behavior of DNA helicases (38,39). We verified this by using a modified labeling scheme, in which the Cy3 and Cy5 dyes were placed in the middle of the 3′ and 5′ overhangs. Similar repetitive unwinding signals were also observed (Supplementary Figure S1), but with noisier FRET signals. The noises arose from the fact that, after the complete rezipping of the displaced strands, Pif1 was still working on the substrate, either translocating along one ssDNA strand or hopping between the two strands (25).

Given that our experiments were performed in the absence of free proteins, the repetitive unwinding should therefore have resulted from the action of a single complex, that is, a Pif1 monomer. This conjecture was verified by the observation of single-step photobleaching of Cy3-labeled Pif1 (see Supplementary Figure S2). In addition, we also observed unwinding signals similar to those for a forked DNA structure, which indicates that the Pif1 monomers bound to the forks rather than the poly(dT) overhangs after the free proteins were removed from the flow chamber. This assumption about the binding position is reasonable given that the affinity of Pif1 for poly(dT) is much lower than that for forked DNA structures (13). For a DNA duplex with a 3′ overhang, it has been observed that a Pif1 monomer binds to the ss/dsDNA junction and reels in the 3′ overhang repetitively for a long time (25). However, it should be noted that our results do not exclude the possibility that a dimer is required for other DNA structures or under other buffer conditions. For example, Zhou *et al*. observed that a Pif1 monomer unwound an RNA–DNA hybrid but did not unwind the duplex in an ssDNA/dsDNA hybrid (25).

To make a further quantitative comparison, we analyzed the fraction of different DNA molecules that were unwound. We used a higher Pif1 concentration (20 nM) for incubation (free proteins were then washed away, just as before) in the experiments in order to have enough DNA molecules being bound with Pif1 and to observe the unwinding events more frequently. As shown in Figure 1F, ∼25% of the forked DNA molecules could be unwound, but only ∼1% of the 5′-tailed DNA molecules were unwound under the same conditions.

The observed phenomena reveal several features of Pif1 in unwinding DNA. (i) A single Pif1 helicase unwinds the forked DNA repetitively with each cycle, being composed of an unwinding process and a rezipping process that resets the DNA substrate to its original state. (ii) Pif1 can only unwind the DNA duplex partially in each cycle, with the lowest FRET values being around 0.4, and thus should have a low unwinding processivity, consistent with previous observations (16). (iii) Pif1 remains bound to the DNA substrate for a long time, because of its high binding affinity for DNA (13). To exclude the possibility that the low unwinding processivity may have been caused by the proximity of the immobilizing surface, we also tethered the DNA substrate to the surface via an ssDNA overhang so that the duplex remained far away from the surface during the unwinding processes. It turned out that Pif1 still exhibited low unwinding processivity (Supplementary Figure S3), as before.

To see the unwinding behaviors of Pif1 in more details, we carried out FRET experiments at different ATP concentrations. It was found that although the unwinding rate decreased with the decreasing of ATP concentration, the unwinding length did not significantly vary (Figure 1C–E), implying that the unwinding termination is independent of the unwinding rate of Pif1 and therefore not determined by a time-dependent stochastic process. In addition, at low ATP concentrations, Pif1 sometimes did not unwind DNA continuously, but with some pauses, reflecting the stepwise unwinding behavior of Pif1.

In the presence of a force, the unwinding length is sensitive to the ATP concentration and the force

To study the effect of force on the DNA unwinding of Pif1, we performed single-molecule DNA unwinding assays using MT. A magnetic bead was tethered to the bottom surface of a flow chamber through two duplex handles (Figure 2A). The local structure of the part of the DNA where Pif1 initiated the hairpin unwinding is the same as that of the forked DNA. The hairpin is stable under an external stretching force of less than 14 pN. Above 14 pN, the DNA extension increases abruptly as the hairpin is unzipped by the force (40). When a Pif1 molecule is loaded to the 26-nt 5′-ssDNA gap and unwinds the hairpin, 2 nucleotides (nt) are released per base pair (bp) unwound, leading to an increase of the DNA extension.

As in the FRET assay, after incubation of the DNA with 2 nM Pif1 for 5 min, we flushed away the free proteins with 600 μl reaction buffer. Upon unwinding initiation after adding ATP, unwinding bursts appeared immediately. A typical unwinding trace is shown in Figure 2B, which looks similar to that in the FRET assay except that the unwinding lengths (heights of unwinding bursts) are generally very long, sometimes exceeding 150 bp. We found that the un-

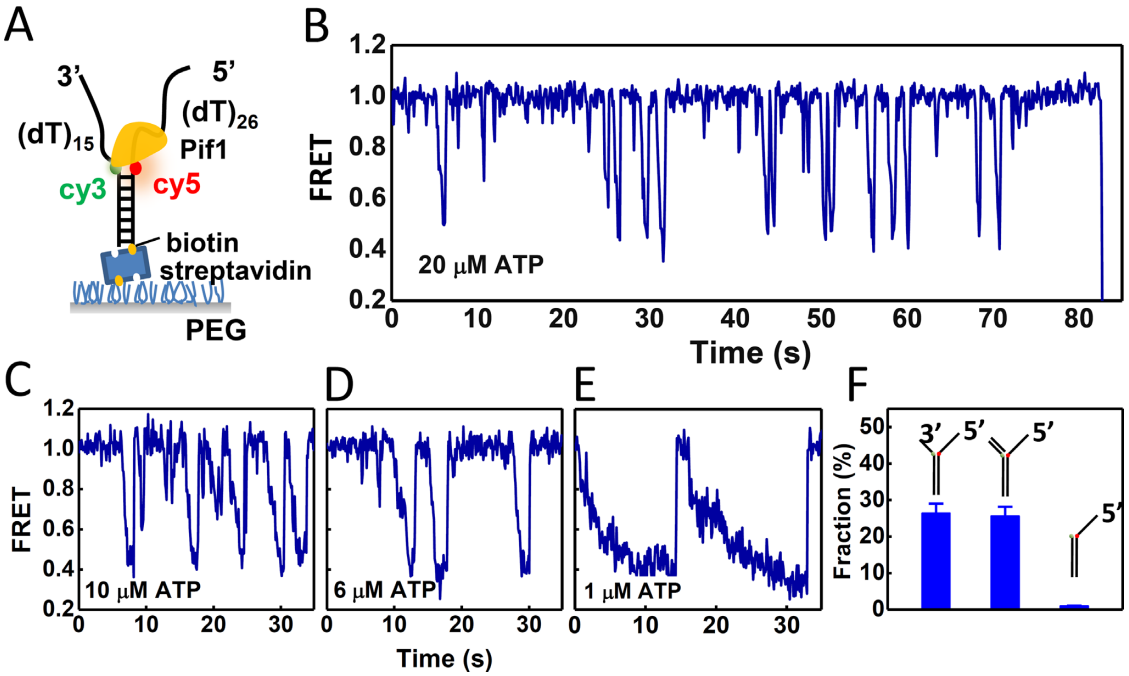

Figure 1. Observation of Pif1-catalyzed DNA unwinding with smRRET assay. (**A**) Schematic illustration of the structure of the 40-bp forked duplex DNA substrate. The donor (Cy3) and acceptor (Cy5) fluorescent molecules are attached at the ss/dsDNA junction. The DNA substrate is tethered to the PEG-coated quartz surface with biotin. (**B–E**) Typical smFRET time traces at different ATP concentrations. A 2 nM Pif1 was used for preincubation with DNA molecules. (**F**) Fraction of DNA molecules unwound among all observable DNA molecules on the coverslip surface. The structures of the DNA molecules (insets) are the same as that shown in (A) or modified. A 20 nM Pif1 was used for preincubation with DNA molecules in each case.

winding length was very sensitive to both the ATP concentration and the force exerted. Typical traces obtained at different forces and ATP concentrations are shown in Figure 2C. The results show clearly that the unwinding length is enhanced by the force at a fixed ATP concentration, or by the ATP concentration at a fixed nonzero force. The force was tuned between ∼8 to ∼2 pN in our experiments. When the force was further lowered to below 2 pN, for example, to 1 pN, the Brownian motion of the magnetic bead became so serious that any useful unwinding signals were buried in the noise.

Unwinding process may include several successive phases

Upon close examination, the unwinding traces of Pif1 in the MT assay can be observed to exhibit diverse patterns. When both the force and the ATP concentration were low, the unwinding traces showed simple sawtooth patterns with short unwinding bursts. However, as the force and/or the ATP concentration were increased, the unwinding process showed a tendency to become composed of several successive unwinding phases that were separated by partial rezipping events. We introduced two parameters, the single-phase unwinding length and the total unwinding length, to quantify the unwinding processes (Figure 2C, last panel). The former is defined as the unwinding length in an uninterrupted unwinding event, that is, a straight segment in the unwinding process; the latter corresponds to the whole unwinding length in an unwinding process, or the peak height of an unwinding burst. The total unwinding length showed a tendency to become very long and sometimes was only limited by the hairpin length (270 bp) of the DNA substrate.

Figure 3A shows the representative histograms of the single-phase unwinding length at different forces. They can be fitted with exponential functions to yield the characteristic lengths. Because the data counts of the first two columns were underestimated due to the signal noises, they were neglected in the fittings. The resultant characteristic single-phase unwinding length increased moderately with the force at fixed ATP concentrations (Figure 4A). When the force was increased from 2 to 7.5 pN at 100 μM ATP, the single-phase unwinding length was enhanced by about 3-fold (from ∼10 to 31 bp). Figure 3B shows the representative histograms of the total unwinding lengths at various forces. For the data acquired at high forces, underestimation of the data counts is not problematic because the noises are reduced. The distributions cannot be fitted by a simple function, neither a single exponential function nor a double exponential function (with a rise and a decay). This is, however, understandable because a total unwinding length is usually a sum of many single-phase unwinding lengths. The average total unwinding length can then be obtained by simply averaging the data. Compared with the single-phase unwinding length, the total unwinding length increased even more significantly with the force (Figure 4A), which is consistent with the obvious trend shown by the unwinding traces in Figure 2C. At a given force, the characteristic single-phase unwinding length was independent of the ATP concentration (Figure 4B) although the total unwinding length increased with the ATP concentration (Figure 2C). Note that, at forces lower than 5 pN, the single-phase

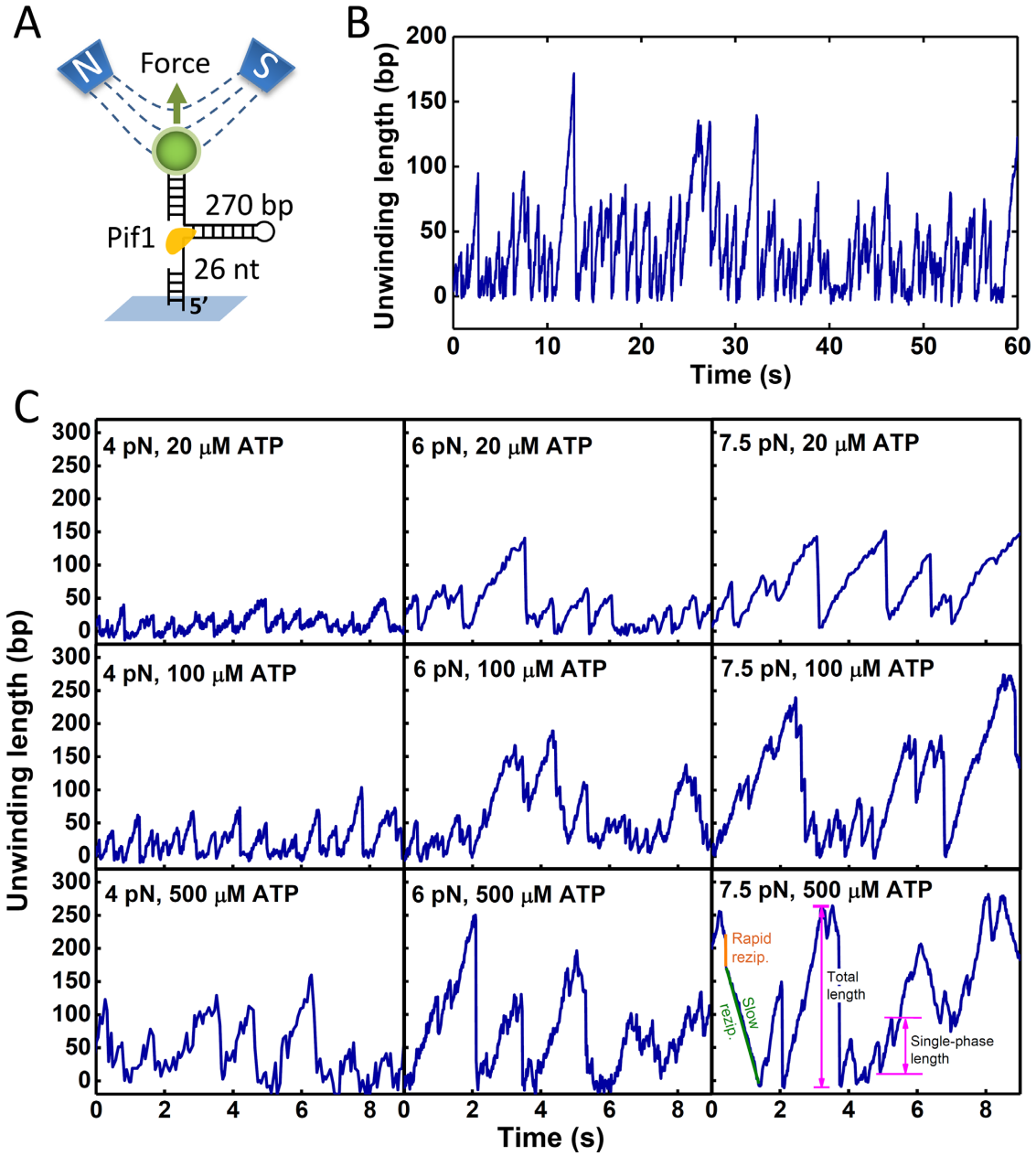

Figure 2. Observation of Pif1-catalyzed DNA unwinding with MT. (**A**) Schematic illustration of the structure and attachment of the DNA construct. A magnetic bead was tethered to the bottom surface of a flow chamber through two duplex handles of the DNA construct with a 270-bp hairpin. The substrate was constructed with a 26-nt 5′ single-stranded gap for the binding of Pif1. The Pif1 concentration during preincubation with the DNA substrates was 2 nM. (**B**) A time trace of the DNA unwinding length at 5 pN force and 100 μM ATP. (**C**) Representative time traces of DNA unwinding at different forces and ATP concentrations. In the last panel, the different parameters and rezipping processes described in the text are defined.

and the total unwinding lengths are essentially the same, reflecting the fact that the unwinding processes mainly consist of a single unwinding phase when the force is low.

In the FRET assay, the two tails of the forked DNA were free of tension, and the unwinding burst of Pif1 exhibited a single unwinding phase only. The results mentioned above can thus explain why the DNA unwinding length of Pif1 is short and does not vary with the ATP concentration in the FRET assay (see Figure 1). In addition, by extrapolating the data in Figure 4A to zero force, we can estimate that the single-phase unwinding length at zero force is lower than 10 bp, which is consistent with that obtained in bulk assays (16). It is noteworthy that in the cases when the ATP concentrations are very low, the unwinding processes that are composed of obvious steps in the FRET assay (Figure 1) should still belong to single-phased ones, rather than multiphased ones.

Rezipping process may consist of two different phases

In addition to the unusual unwinding kinetics, interesting features were also noticed for the rezipping processes in the

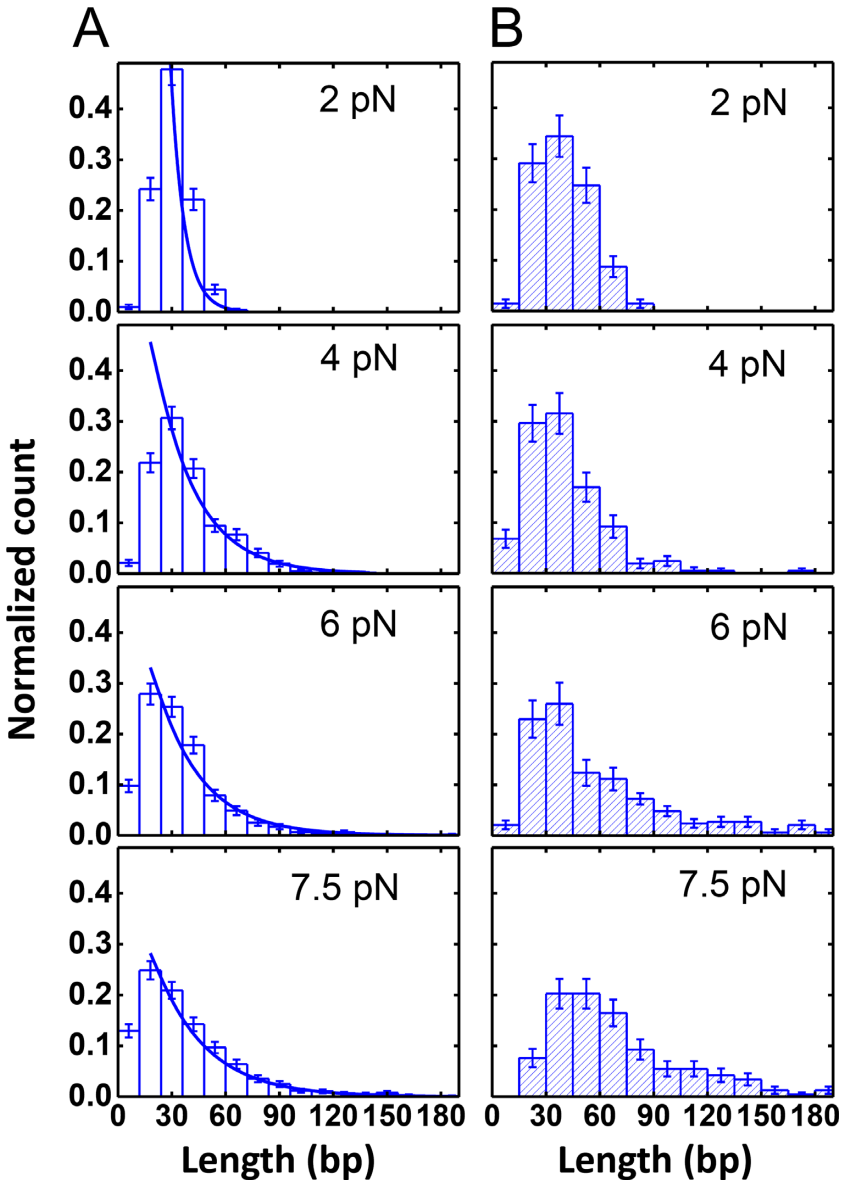

Figure 3. Representative histograms of the single-phase and total unwinding lengths at different forces. (**A**) Single-phase unwinding length at 100 μM ATP. The solid lines are exponential fittings of the data (the first two columns were neglected in each fitting as they were underestimated due to signal noise). (**B**) Total unwinding length at 100 μM ATP. All error bars are SEM representing the statistical error in the bins ($N = 500$, 200 for single-phase and for total unwinding lengths, respectively).

observed unwinding bursts. At low forces and low ATP concentrations, a rezipping process in an unwinding burst consisted of a single abrupt phase only. When the force and/or the ATP concentration became higher, the rezipping process could consist of both rapid and slow phases, with the sequence of occurrence not fixed (see, e.g. the last panel Figure 2C). The existence of the slow rezipping phase indicates that Pif1 may translocate on the displaced 3′ strand during the re-annealing of the two separated strands. This argument is supported by three factors: (i) the Pif1 helicase has a 5′-3′ directionality and is thus unlikely to slide back slowly on the 5′ tracking strand; (ii) the slow rezipping rate (in bp/s) is almost the same as the duplex unwinding rate; (iii) the slow and rapid rezipping phases appear alternately (see the last panel in Figure 2C).

We also analyzed the dependence of the proportion of the slow rezipping phase on the force and the ATP concentration (Figure 4C and D). At a fixed (high) ATP concentration, the proportion of the slow rezipping phase remained negligible at low forces and then increased significantly as the force was increased to ∼6 pN and beyond; at a fixed (high) force, it increased continuously with the ATP concentration. As shown clearly in Figure 4C, a force larger than ∼6 pN is critical for the slow rezipping events to occur frequently.

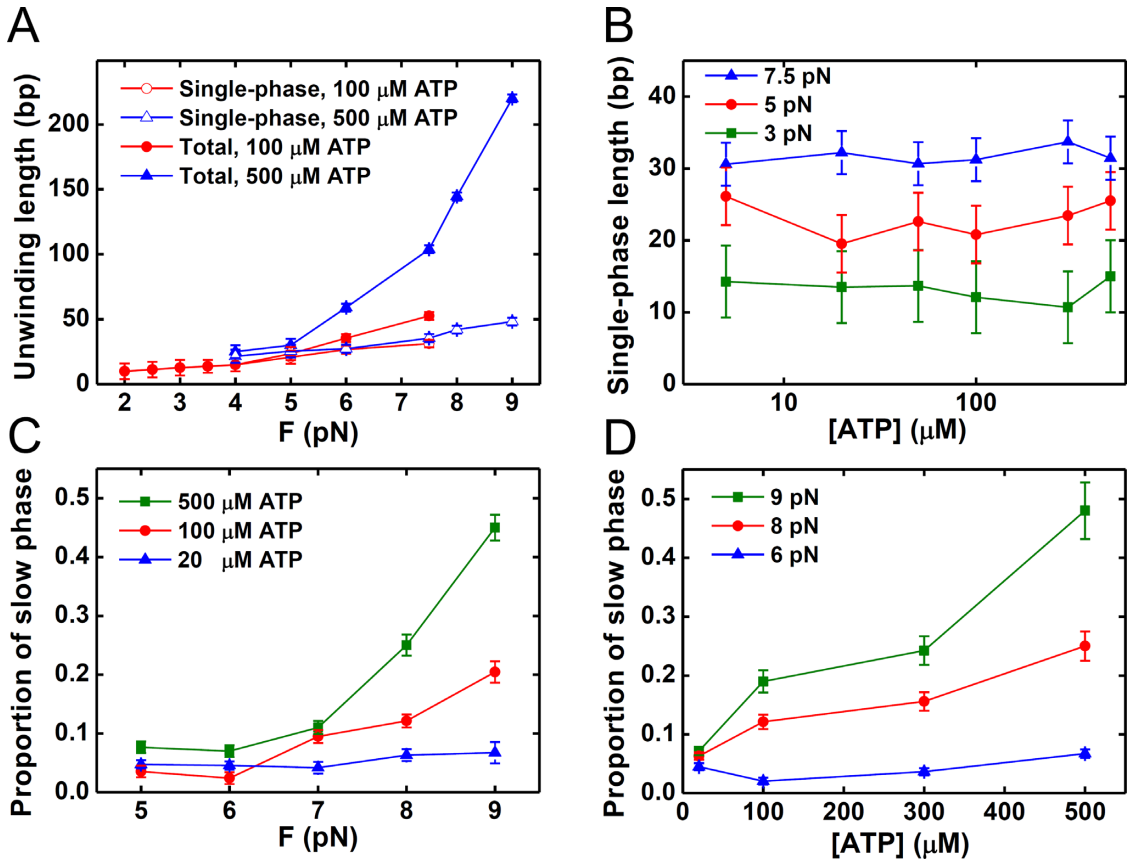

Figure 4. Dependences of the unwinding lengths and the rezipping process on force and ATP concentration. (**A**) Characteristic single-phase and average total unwinding lengths versus force at 100 and 500 μM ATP. (**B**) Characteristic single-phase unwinding length versus ATP concentration at different forces. Error bars are SD representing fitting error. (**C, D**) Proportion of the slow rezipping phases in all abrupt and slow phases versus force (C) and ATP concentration (D). Error bars denote SD.

Unwinding rate is enhanced by force

To understand the DNA unwinding mechanism of Pif1, it is important to determine the effect of force on the unwinding rate. To exclude uncertainties that may arise from converting the DNA extension increment to the number of base pairs unwound at different forces, we measured the unwinding rate of a short hairpin of 40 bp at a slightly higher Pif1 concentration (20 nM). The substrate design and a trace of the raw data are shown in Supplementary Figure S4. The unwinding of the hairpin was not only complete, but also uninterrupted by any rezipping event. The unwinding rate was hence directly calculated by dividing the number of base pairs of the hairpin by the unwinding time. Two representative distributions of the unwinding rates are given in Figure 5A. The averages of the unwinding rates thus obtained at different forces are listed in Figure 5B, from which one can see that the averaged unwinding rate is significantly enhanced by the force, with the rate at 5 pN being as much as 3-fold of that at zero force.

DISCUSSION

Our experimental results suggest that Pif1 is an energetic helicase, which can unwind a forked DNA duplex repetitively. It has a high affinity for the forked DNA structure and does not detach from the substrate easily, but loosens its strong association with the tracking strand frequently. Although Pif1 does not unwind effectively a 5′ tailed DNA duplex, it can unwind a forked DNA duplex. Our results, nonetheless, seem to contradict those of previous studies (16). However, in light of the detailed behaviors of Pif1 observed at the single-molecule level, this contradiction can be easily resolved. The previous studies were performed in bulk assays. Although Pif1 can unwind a forked duplex DNA, repetitively, the single-phase unwinding length, or equivalently the processivity, is less than 10 bp at zero force. Thus, in these bulk assays where the lengths of the DNA duplexes were usually longer than 10 bp, no DNA unwinding could be observed phenomenally unless the Pif1 concentration was so high that two or more Pif1 molecules could bind to the displaced ssDNA tails to eliminate the rezipping. Under this condition, successive unwinding by several monomers could extend the effective processivity of Pif1.

The novel unwinding features of Pif1 as observed in this study are summarized as follows: (i) Pif1 unwinds a forked DNA repetitively; (ii) the single-phase unwinding length is independent of the ATP concentration at a fixed force (including zero force); (iii) Pif1 unwinds more base pairs in a single unwinding phase when the force exerted on the forked DNA is increased; (iv) the unwinding process consists of

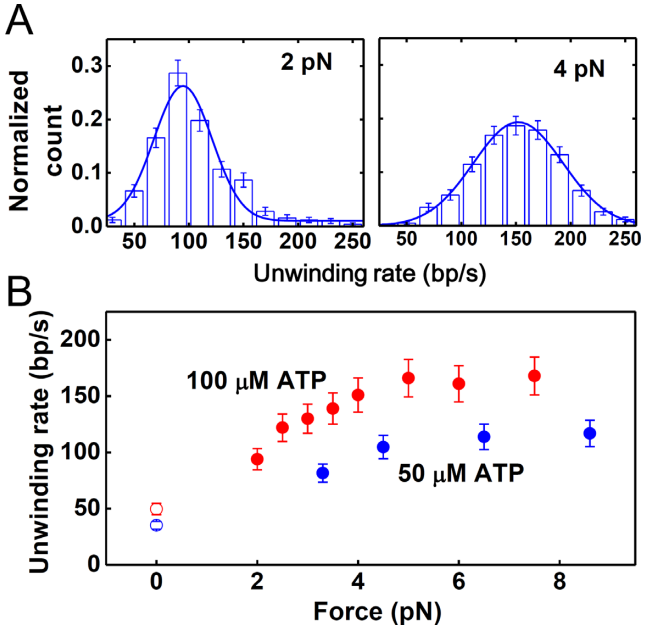

Figure 5. Dependence of the DNA unwinding rate on force. (**A**) Representative histograms of the unwinding rate at different forces. The Pif1 concentration during the preincubation with DNA substrates was 2 nM. The ATP concentration used for the unwinding initiation was 100 μM. The solid lines are the Gaussian fittings that give the average unwinding rates shown below. Error bars are SEM representing statistical error ($N = 500$). (**B**) Average unwinding rate versus force at 50 and 100 μM ATP. The data points at zero force are obtained from smFRET experiments. Error bars denote SD.

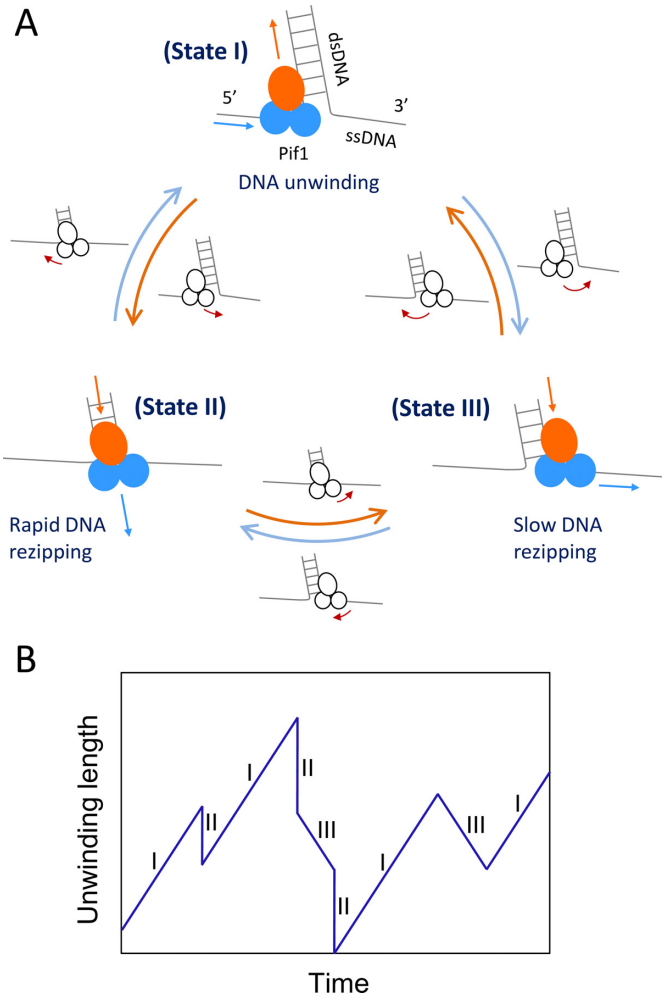

Figure 6. Model for the repetitive DNA unwinding by Pif1. (**A**) There exist three different states in which Pif1 interacts with the DNA substrate. In State I, which corresponds to DNA unwinding, Pif1 binds both the 5′ tracking strand, through the two RecA-like domains (blue), and the DNA duplex at the ss/dsDNA junction. In addition, it also has some interaction with the 3′ strand. In State II, Pif1 continues to interact weakly with the displaced 3′ strand after loosening its strong association with the 5′ tracking strand; the tracking and displaced ssDNA strands rezip rapidly and push Pif1 backward with the retreating ss/dsDNA junction. In State III, Pif1 becomes, after loosening its strong association with the 5′ tracking strand, bound firmly to the 3′ displaced strand and then translocates along it. In this case, the tracking and displaced ssDNA strands rezip in a relatively slow manner that is determined by the ATP-dependent ssDNA translocation rate of Pif1. As indicated by the arrows, interconversion may occur between any two of the three states (or processes) during the repetitive unwinding of forked DNA by Pif1 (see the main text for details). (**B**) Schematic diagram illustrating the unwinding patterns due to the existence of three states of Pif1, as observable in the experiments.

several successive unwinding phases at high forces and high ATP concentrations, ultimately resulting in a long total unwinding length; (v) it becomes more probable for Pif1 to translocate on the 3′ displaced ssDNA during the rezipping process at high forces and high ATP concentrations; (vi) and the unwinding rate increases with the force.

Based on the above results, we propose a simple kinetic model for the DNA unwinding activity of Pif1 (Figure 6A). In this model, Pif1 may interact with its substrate in three different states. In the unwinding state (State I), Pif1 interacts with the DNA duplex at the ss/dsDNA junction as well as the 5′ tracking strand. The former is ATP-independent and strong, whereas the latter depends on the nucleotide state and may become weak during an ATP hydrolysis cycle. In addition, considering the fact that Pif1 prefers forked rather than nonforked DNA structures (14–16), we assume that Pif1 may also have some weak interaction with the 3′ strand. During DNA unwinding, Pif1 may loosen its strong association with the 5′ tracking strand at a certain stage of the ATP hydrolysis cycle and thus make state transition from State I to State II. In State II, Pif1 binds loosely to both the 5′ and 3′ strands while remaining associated with the ss/dsDNA junction, and thus may slide backward as it is pushed by the retreating ss/dsDNA junction when the two displaced ssDNA strands rezip rapidly. During the slippage in State II, Pif1 may rebind strongly to the 5′ strand to unwind the duplex again (41–43). Alternatively, it may bind strongly to the 3′ strand, thus making strand switching (44) and entering the third state, State III. In State III, Pif1 translocates (driven by ATP hydrolysis) along the 3′ ssDNA and the two displaced ssDNA strands rezip at a rate that is determined by the ssDNA translocation rate of Pif1. It is noteworthy that, in our model, state transition may occur between any two of the three states during the repetitive unwinding of forked DNA. This explains the transitions between any two of the three processes (unwinding, rapid DNA rezipping and slow DNA rezipping) in the unwinding traces in our MT assay (Figure 6B).

This model can explain the effect of force on the unwinding of Pif1. At low forces, after Pif1 loosens its strong association with the 5′ tracking strand (from State I to State II), the rezipping process completes so quickly that the ss/dsDNA junction may have already retreated to its original position before the helicase can bind firmly to the displaced 3′ strand; at the end of the rezipping, the helicase rebinds to the tracking strand and starts to unwind the duplex again (from State II to State I). The unwinding thus has only a single phase and the total unwinding length or the processivity is the same as the single-phase unwinding length. Pincus *et al*. (45) proposed a theory explaining why the helicase's processivity always increases with force. This theory can be adopted to explain the slight enhancement of the single-phase unwinding length of Pif1 with force. At high forces, the rezipping process is not energetically favorable, and it takes a longer time for the two strands to rezip; thus, after loosening its strong association with the 5′ tracking strand, Pif1 has time to bind firmly to and (then) translocate along the 3′ displaced strand (from State I to State III), yielding the slow rezipping phase. The slow rezipping may proceed all the way to the end. However, if Pif1 loosens its firm binding to the 3′ displaced strand during the slow rezipping process, a quick rezipping phase (from State III to State II) or an unwinding phase (from State III to State I) may follow. On the other hand, because the rezipping process is not energetically favorable at high forces, another event may also happen: during the rezipping process (State II), Pif1 has an increased probability to rebind the tracking strand to reinitiate a new unwind phase (from State II to State I) before the rezipping is completed. Therefore, the DNA unwinding process may consist of several successive phases, and the lengths of these phases all contribute to the total unwinding length. The large enhancement of the total unwinding length by the force can then be attributed to the increase of the probability of Pif1's rebinding the track strand.

Beside the unwinding length, we observed that the unwinding rate of Pif1 was also enhanced by force. Some ring-shaped replicative helicases, for example, T7 and T4 gp41, were also observed to exhibit such enhancement (46,47). Pif1 is a non-ring-shaped helicase. So far, no other non-ring-shaped superfamily 1 and 2 helicases have been reported to have a force-enhanced unwinding rate. In the absence of crystal structures of Pif1-DNA complexes, we are not able to give a clear explanation of the enhancement. However, we could argue that the enhancement may be due to the releasing of partial wrapping of ssDNA around Pif1, as has been previously proposed (22). The ssDNA wrapped on the surface of Pif1 may hamper the translocation of the helicase; a force may strip off the ssDNA to facilitate the translocation and thus enhance the unwinding rate.

We conclude with a discussion about the relevance of the force effects to the cellular functions of Pif1. As mentioned in the Introduction section, Pif1 plays a role in both OFM and BIR, which require quite different unwinding lengths. Our results can explain why Pif1 can function in both processes. In the former process, there is no force on the DNA structure and thus Pif1 has a very limited unwinding length/processivity. However, in the latter process, a migrating D-loop structure is involved (32). Because the end-to-end distance of a dsDNA is longer than that of an ssDNA at low forces (48), the stiff dsDNA in the D-loop has to be bent and thus applies a force on the ssDNA. Under physiological conditions, the extension of ssDNA equals that of dsDNA when subjected to a force of ∼7 pN (36), therefore the stiff dsDNA in a D-loop structure may exert a force up to 7 pN on the flexible ssDNA as long as the D-loop is not large. As the enhancement of the total DNA unwinding length becomes obvious at > 6 pN (see Figure 4A), the D-loop structure thus enables Pif1 to work effectively in the process of BIR.

SUPPLEMENTARY DATA

Supplementary Data are available at NAR Online.

FUNDING

National Natural Science Foundation of China [61275192, 11574382, 11574381]; Funding for open access charge: National Natural Science Foundation of China [61275192]; International associated laboratory (LIA) 'G-quadruplex-HELI' (CNRS, ENS-Cachan, Institute of Physics of the Chinese Academy of Sciences) (in part).
Conflict of interest statement. None declared.

REFERENCES

1. Patel,S.S. and Donmez,I. (2006) Mechanisms of helicases. *J. Biol. Chem.*, **281**, 18265–18268.
2. Singleton,M.R., Dillingham,M.S. and Wigley,D.B. (2007) Structure and mechanism of helicases and nucleic acid translocases. *Annu. Rev. Biochem.*, **76**, 23–50.
3. Lohman,T.M., Tomko,E.J. and Wu,C.G. (2008) Non-hexameric DNA helicases and translocases: mechanisms and regulation. *Nat. Rev. Mol. Cell Biol.*, **9**, 391–401.
4. Wu,Y. (2012) Unwinding and rewinding: double faces of helicase? *J. Nucleic Acids*, **2012**, 140601.
5. Patel,S.S. and Picha,K.M. (2000) Structure and function of hexameric helicases. *Annu. Rev. Biochem.*, **69**, 651–697.
6. Singleton,M.R. and Wigley,D.B. (2002) Modularity and specialization in superfamily 1 and 2 helicases. *J. Bacteriol.*, **184**, 1819–1826.
7. Hickson,I.D. (2003) RecQ helicases: caretakers of the genome. *Nat. Rev. Cancer*, **3**, 169–178.
8. Delagoutte,E. and von Hippel,P.H. (2003) Helicase mechanisms and the coupling of helicases within macromolecular machines. Part II: Integration of helicases into cellular processes. *Q. Rev. Biophys.*, **36**, 1–69.
9. Bessler,J.B., Torres,J.Z. and Zakian,V.A. (2001) The Pif1p subfamily of helicases: region-specific DNA helicases? *Trends Cell Biol.*, **11**, 60–65.
10. Bochman,M.L., Sabouri,N. and Zakian,V.A. (2010) Unwinding the functions of the Pif1 family helicases. *DNA Rep.*, **9**, 237–249.
11. Boule,J.B. and Zakian,V.A. (2006) Roles of Pif1-like helicases in the maintenance of genomic stability. *Nucleic Acids Res.*, **34**, 4147–4153.
12. Bochman,M.L., Judge,C.P. and Zakian,V.A. (2011) The Pif1 family in prokaryotes: what are our helicases doing in your bacteria? *Mol. Biol. Cell*, **22**, 1955–1959.
13. Paeschke,K., Bochman,M.L., Garcia,P.D., Cejka,P., Friedman,K.L., Kowalczykowski,S.C. and Zakian,V.A. (2013) Pif1 family helicases suppress genome instability at G-quadruplex motifs. *Nature*, **497**, 458–462.
14. Lahaye,A., Leterme,S. and Foury,F. (1993) PIF1 DNA helicase from Saccharomyces cerevisiae. Biochemical characterization of the enzyme. *J. Biol. Chem.*, **268**, 26155–26161.
15. Boule,J.B. and Zakian,V.A. (2007) The yeast Pif1p DNA helicase preferentially unwinds RNA DNA substrates. *Nucleic Acids Res.*, **35**, 5809–5818.

16. Ramanagoudr-Bhojappa,R., Chib,S., Byrd,A.K., Aarattuthodiyil,S., Pandey,M., Patel,S.S. and Raney,K.D. (2013) Yeast Pif1 helicase exhibits a one-base-pair stepping mechanism for unwinding duplex DNA. *J. Biol. Chem.*, **288**, 16185–16195.
17. Schulz,V.P. and Zakian,V.A. (1994) The saccharomyces PIF1 DNA helicase inhibits telomere elongation and de novo telomere formation. *Cell*, **76**, 145–155.
18. Zhou,J.Q. (2000) Pif1p Helicase, a Catalytic Inhibitor of Telomerase in Yeast. *Science*, **289**, 771–774.
19. Makovets,S. and Blackburn,E.H. (2009) DNA damage signalling prevents deleterious telomere addition at DNA breaks. *Nat. Cell Biol.*, **11**, 1383–1386.
20. Paeschke,K., Capra,J.A. and Zakian,V.A. (2011) DNA replication through G-quadruplex motifs is promoted by the Saccharomyces cerevisiae Pif1 DNA helicase. *Cell*, **145**, 678–691.
21. Barranco-Medina,S. and Galletto,R. (2010) DNA binding induces dimerization of Saccharomyces cerevisiae Pif1. *Biochemistry*, **49**, 8445–8454.
22. Galletto,R. and Tomko,E.J. (2013) Translocation of Saccharomyces cerevisiae Pif1 helicase monomers on single-stranded DNA. *Nucleic Acids Res.*, **41**, 4613–4627.
23. Mateyak,M.K. and Zakian,V.A. (2006) Human PIF helicase is cell cycle regulated and associates with telomerase. *Cell Cycle*, **5**, 2796–2804.
24. Chang,M., Luke,B., Kraft,C., Li,Z., Peter,M., Lingner,J. and Rothstein,R. (2009) Telomerase is essential to alleviate pif1-induced replication stress at telomeres. *Genetics*, **183**, 779–791.
25. Zhou,R., Zhang,J., Bochman,M.L., Zakian,V.A. and Ha,T. (2014) Periodic DNA patrolling underlies diverse functions of Pif1 on R-loops and G-rich DNA. *eLife*, **3**, e02190.
26. Ryu,G.H., Tanaka,H., Kim,D.H., Kim,J.H., Bae,S.H., Kwon,Y.N., Rhee,J.S., MacNeill,S.A. and Seo,Y.S. (2004) Genetic and biochemical analyses of Pfh1 DNA helicase function in fission yeast. *Nucleic Acids Res.*, **32**, 4205–4216.
27. Budd,M.E., Reis,C.C., Smith,S., Myung,K. and Campbell,J.L. (2006) Evidence suggesting that Pif1 helicase functions in DNA replication with the Dna2 helicase/nuclease and DNA polymerase delta. *Mol. Cell. Biol.*, **26**, 2490–2500.
28. Rossi,M.L., Pike,J.E., Wang,W., Burgers,P.M., Campbell,J.L. and Bambara,R.A. (2008) Pif1 helicase directs eukaryotic Okazaki fragments toward the two-nuclease cleavage pathway for primer removal. *J. Biol. Chem.*, **283**, 27483–27493.
29. Stith,C.M., Sterling,J., Resnick,M.A., Gordenin,D.A. and Burgers,P.M. (2008) Flexibility of eukaryotic Okazaki fragment maturation through regulated strand displacement synthesis. *J. Biol. Chem.*, **283**, 34129–34140.
30. Pike,J.E., Burgers,P.M., Campbell,J.L. and Bambara,R.A. (2009) Pif1 helicase lengthens some Okazaki fragment flaps necessitating Dna2 nuclease/helicase action in the two-nuclease processing pathway. *J. Biol. Chem.*, **284**, 25170–25180.
31. Pike,J.E., Henry,R.A., Burgers,P.M., Campbell,J.L. and Bambara,R.A. (2010) An alternative pathway for Okazaki fragment processing: resolution of fold-back flaps by Pif1 helicase. *J. Biol. Chem.*, **285**, 41712–41723.
32. Wilson,M.A., Kwon,Y., Xu,Y., Chung,W.H., Chi,P., Niu,H., Mayle,R., Chen,X., Malkova,A., Sung,P. and Ira,G. (2013) Pif1 helicase and Poldelta promote recombination-coupled DNA synthesis via bubble migration. *Nature*, **502**, 393–396.
33. Saini,N., Ramakrishnan,S., Elango,R., Ayyar,S., Zhang,Y., Deem,A., Ira,G., Haber,J.E., Lobachev,K.S. and Malkova,A. (2013) Migrating bubble during break-induced replication drives conservative DNA synthesis. *Nature*, **502**, 389–392.
34. Roy,R., Hohng,S. and Ha,T. (2008) A practical guide to single-molecule FRET. *Nat. Methods*, **5**, 507–516.
35. Wang,S., Qin,W., Li,J.H., Lu,Y., Lu,K.Y., Nong,D.G., Dou,S.X., Xu,C.H., Xi,X.G. and Li,M. (2015) Unwinding forward and sliding back: an intermittent unwinding mode of the BLM helicase. *Nucleic Acids Res.*, **43**, 3736–3746.
36. Strick,T.R., Allemand,J.F., Bensimon,D., Bensimon,A. and Croquette,V. (1996) The elasticity of a single supercoiled DNA molecule. *Science*, **271**, 1835–1837.
37. Smith,S.B., Cui,Y. and Bustamante,C. (1996) Overstretching B-DNA: the elastic response of individual double-stranded and single-stranded DNA molecules. *Science*, **271**, 795–799.
38. Pandey,M., Syed,S., Donmez,I., Patel,G., Ha,T. and Patel,S.S. (2009) Coordinating DNA replication by means of priming loop and differential synthesis rate. *Nature*, **462**, 940–943.
39. Syed,S., Pandey,M., Patel,S.S. and Ha,T. (2014) Single-molecule fluorescence reveals the unwinding stepping mechanism of replicative helicase. *Cell Rep.*, **6**, 1037–1045.
40. Essevaz-Roulet,B., Bockelmann,U. and Heslot,F. (1997) Mechanical separation of the complementary strands of DNA. *Proc. Natl. Acad. Sci. U.S.A.*, **94**, 11935–11940.
41. Lee,S.J., Syed,S., Enemark,E.J., Schuck,S., Stenlund,A., Ha,T. and Joshua-Tor,L. (2014) Dynamic look at DNA unwinding by a replicative helicase. *Proc. Natl. Acad. Sci. U.S.A.*, **111**, E827–E835.
42. Manosas,M., Spiering,M.M., Zhuang,Z., Benkovic,S.J. and Croquette,V. (2009) Coupling DNA unwinding activity with primer synthesis in the bacteriophage T4 primosome. *Nat. Chem. Biol.*, **5**, 904–912.
43. Sun,B., Johnson,D.S., Patel,G., Smith,B.Y., Pandey,M., Patel,S.S. and Wang,M.D. (2011) ATP-induced helicase slippage reveals highly coordinated subunits. *Nature*, **478**, 132–135.
44. Dessinges,M.N., Lionnet,T., Xi,X.G., Bensimon,D. and Croquette,V. (2004) Single-molecule assay reveals strand switching and enhanced processivity of UvrD. *Proc. Natl. Acad. Sci. U.S.A.*, **101**, 6439–6444.
45. Pincus,D.L., Chakrabarti,S. and Thirumalai,D. (2015) Helicase processivity and not the unwinding velocity exhibits universal increase with force. *Biophys. J.*, **109**, 220–230.
46. Johnson,D.S., Bai,L., Smith,B.Y., Patel,S.S. and Wang,M.D. (2007) Single-molecule studies reveal dynamics of DNA unwinding by the ring-shaped T7 helicase. *Cell*, **129**, 1299–1309.
47. Lionnet,T., Spiering,M.M., Benkovic,S.J., Bensimon,D. and Croquette,V. (2007) Real-time observation of bacteriophage T4 gp41 helicase reveals an unwinding mechanism. *Proc. Natl. Acad. Sci. U.S.A.*, **104**, 19790–19795.
48. Huber,M.D., Duquette,M.L., Shiels,J.C. and Maizels,N. (2006) A conserved G4 DNA binding domain in RecQ family helicases. *J. Mol. Biol.*, **358**, 1071–1080.